Available online at www.sciencedirect.com
ScienceDirect
Applied Geochemistry 21 (2006) 1551–1569
Applied Geochemistry
www.elsevier.com/locate/apgeochem

CO_2 emissions and heat flow through soil, fumaroles, and steam heated mud pools at the Reykjanes geothermal area, SW Iceland

Thráinn Fridriksson [a,*], Bjarni Reyr Kristjánsson [a], Halldór Ármannsson [a], Eygerður Margrétardóttir [a], Snjólaug Ólafsdóttir [a], Giovanni Chiodini [b]

[a] *Iceland GeoSurvey, Grensásvegi 9, 108 Reykjavík, Iceland*
[b] *Osservatorio Vesuviano, Instituto Nazionale di Geofisica e Vulcanologia, Via Diocleziano 328, 80124 Napoli, Italy*

Received 5 October 2005; accepted 11 April 2006
Editorial handling by R. Fuge
Available online 20 July 2006

Abstract

Carbon dioxide emissions and heat flow through soil, steam vents and fractures, and steam heated mud pools were determined in the Reykjanes geothermal area, SW Iceland. Soil diffuse degassing of CO_2 was quantified by soil flux measurements on a 600 m by 375 m rectangular grid using a portable closed chamber soil flux meter and the resulting data were analyzed by both a graphical statistical method and sequential Gaussian simulations. The soil temperature was measured in each node of the grid and used to evaluate the heat flow. The heat flow data were also analyzed by sequential Gaussian simulations. Heat flow from steam vents and fractures was determined by quantifying the amount of steam emitted from the vents by direct measurements of steam flow rate. The heat loss from the steam heated mud pools was determined by quantifying the rate of heat loss from the pools by evaporation, convection, and radiation. The steam flow rate into the pools was calculated from the observed heat loss from the pools, assuming that steam flow was the only mechanism of heat transport into the pool. The CO_2 emissions from the steam vents and mud pools were determined by multiplying the steam flow rate from the respective sources by the representative CO_2 concentration of steam in the Reykjanes area. The observed rates of CO_2 emissions through soil, steam vents, and steam heated mud pools amounted to 13.5 ± 1.7, 0.23 ± 0.05, and 0.13 ± 0.03 tons per day, respectively. The heat flow through soil, steam vents, and mud pools was 16.9 ± 1.4, 2.2 ± 0.4, and 1.2 ± 0.1 MW, respectively. Heat loss from the geothermal reservoir, inferred from the CO_2 emissions through the soil amounts to 130 ± 16 MW of thermal energy. The discrepancy between the observed heat loss and the heat loss inferred from the CO_2 emissions is attributed to steam condensation in the subsurface due to interactions with cold ground water. These results demonstrate that soil diffuse degassing can be a more reliable proxy for heat loss from geothermal systems than soil temperatures. The soil diffuse degassing at Reykjanes appears to be strongly controlled by the local tectonics. The observed diffuse degassing defines 3–5 elongated N–S trending zones (000–020°). The orientation of the diffuse degassing structures at Reykjanes is consistent with reported trends of right lateral strike slip faults in the area. The natural CO_2 emissions from Reykjanes under the current low-production conditions are about 16% of the expected emissions from a 100 MWe power plant, which has recently been commissioned at Reykjanes.

* Corresponding author. Fax: +354 528 1699.
E-mail address: thf@isor.is (Th. Fridriksson).

0883-2927/$ - see front matter © 2006 Elsevier Ltd. All rights reserved.
doi:10.1016/j.apgeochem.2006.04.006

1. Introduction

Numerous studies in the last 15 a have shown that globally significant amounts of CO_2 are released to the atmosphere by quiescent degassing of volcanoes and soil diffuse degassing from volcanic geothermal systems (see review papers by Kerrick, 2001; Mörner and Etiope, 2002). It has been demonstrated that soil diffuse degassing on flanks of volcanoes is sensitive to changes in magmatic activity, thus providing a potential, relatively safe method for volcano monitoring. Soil diffuse CO_2 degassing has also been shown to be a good indicator of the energetic state of geothermal systems (Brombach et al., 2001; Chiodini et al., 2001, submitted for publication). This is because CO_2 gas reaches the surface more easily than steam that can condense in the subsurface where groundwater flow can transport the resulting thermal energy laterally out of the systems (Chiodini et al., submitted for publication). These studies have, furthermore, improved our understanding of the natural CO_2 budget of the atmosphere.

Many recent studies of CO_2 emissions from geothermal and volcanic systems have been conducted in areas located on convergent boundaries, such as in South and Central Italy (e.g., Baubron et al., 1991; Allard et al., 1991; Chiodini et al., 1996, 1998, 2001, submitted for publication; Favara et al., 2001; Aiuppa et al., 2004), the Aegean islands (Brombach et al., 2001), Japan (Hernández et al., 2001a,b; Notsu et al., 2005), White Island, New Zealand (Werner et al., 2004) and Central America (Salazar et al., 2001; Lewicki et al., 2003). Several studies have been conducted in hot-spot tectonic settings such as in Yellowstone Park (Werner et al., 2000; Werner and Brantley, 2003), Hawaii (Gerlach et al., 2002), and the Canary Islands (Hernández et al., 1998) and estimates of CO_2 release from the submarine volcanic geothermal systems of the Mid Ocean Ridges have also been reported (Marty and Tolstikhin, 1998). This study complements the growing number of studies on CO_2 emissions from volcanic and geothermal systems world-wide by adding data from Iceland, where the tectonic setting is characterized by coincidence of Mid Ocean Ridge-like extensional tectonics (e.g., Pálmason and Saemundsson, 1974) and a mantle plume hot spot (Wolfe et al., 1997).

Two previous studies have been aimed at determining the CO_2 discharge from Icelandic volcanic/geothermal systems. Ágústsdóttir and Brantley (1994) determined the long term fluxes of volatiles, including CO_2, and heat loss from the Grímsvötn subglacial geothermal system in Vatnajökull SE-Iceland, and Gíslason (2000) reported values for CO_2 release from the glacially capped Eyjafjallajökull caldera. The Grímsvötn volcanic system is the most active volcanic system in Iceland and the associated geothermal system is consequently very powerful. Ágústsdóttir and Brantley (1994) found that in the period between 1954 and 1991 the natural heat release from the system amounted to 4250 MW on average and the CO_2 release to 190,000 tons a^{-1}. The reported rate of CO_2 release from Eyjafjallajökull is much smaller, being in the range from 2600 to 26,000 tons a^{-1} (Gíslason, 2000). The glacial caps on Grímsvötn and Eyjafjallajökull facilitate quantification of the CO_2 release from these systems because all of the CO_2 released from these systems is dissolved in glacial melt water and the CO_2 flux from the system can be determined by measuring the flow rate and composition of the melt water. However, the glacial caps obviously complicate further investigations of the nature of the underlying volcanic/geothermal systems; it is, for instance, not clear whether a hydrothermal system exists under Eyjafjallajökull.

In this communication results are presented of the first survey of soil diffuse degassing from an Icelandic geothermal system as well as measurements of focused degassing via steam vents and steam heated pools. The results provide insights into the tectonic control of ascending geothermal fluids in the system as well as the natural heat flow from the system. Comparison of diffuse CO_2 degassing and heat flow estimates based on soil temperature measurements places constraints on the steam condensation in shallow groundwater currents. The results of this study can also be used to evaluate the relative environmental impact of a planned 100 MWe geothermal power plant in the area by providing pre-development natural CO_2 emissions for comparison to anthropogenic emissions by the power plant and a reference value for future studies of the effect of power production on natural CO_2 emission.

2. Geological settings

The Reykjanes geothermal area is located at the center of the Reykjanes volcanic system (Jakobsson et al., 1978) at the south western tip of the Reykjanes peninsula (see Fig. 1a). This volcanic system

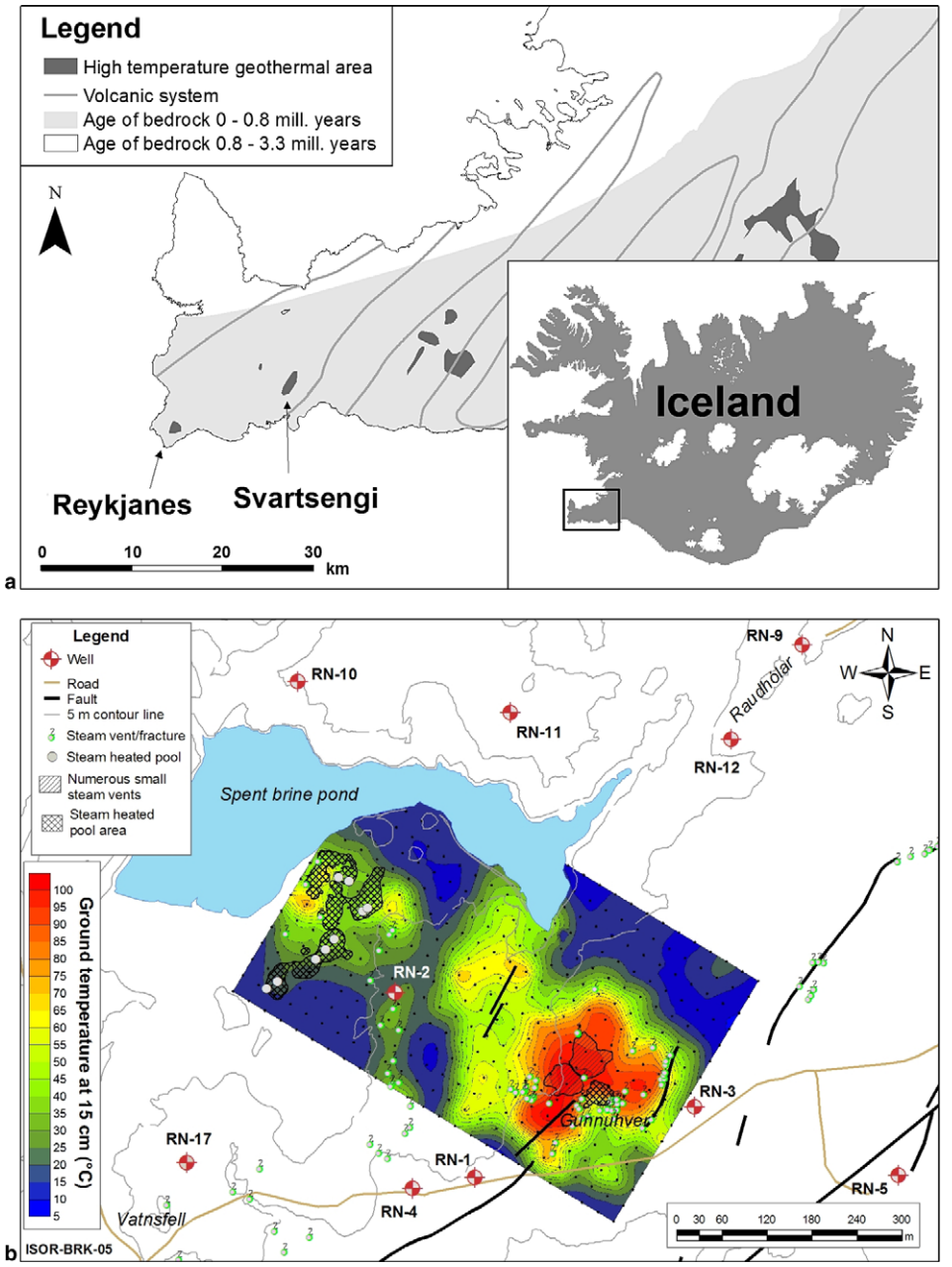

Fig. 1. (a) Map of the Reykjanes peninsula showing the location of the Reykjanes volcanic system (based on Saemundsson and Jóhannesson, 2004) and (b) map of the Reykjanes geothermal area showing surface geothermal manifestations, including steam vents, steam fractures and steam heated pools. Soil temperature at 15 cm depth is shown by filled contour lines in the present study area.

is the westernmost system in Iceland's western neovolcanic zone, which is the subaerial continuation of the Reykjanes Ridge. The Reykjanes volcanic system is characterized by oblique extensional tectonics (Clifton and Schlische, 2003) and episodic fissure eruption volcanism (Jónsson, 1983; Sigurgeirsson, 2004). The two most recent volcanic episodes occurred in the late 12th and the early 13th century and between 1.9 and 2.1 ka ago (Sigurgeirsson, 1995, 2004) and new, unpublished radiocarbon dates indicate that volcanic eruptions occurred at Reykjanes about 3.1 ka ago (K. Saemundsson, personal communication). The landscape is dominated by recent lava flows and volcanic crater rows but a

few Pleistocene hyaloclastite ridges protrude through the younger Holocene lavas.

Twenty-four exploration and production wells have been drilled at Reykjanes to date and drill chip studies have provided important information on the stratigraphy of the geothermal system (Björnsson et al., 1971; Franzson et al., 2002; Franzson, 2004). Holocene lavas extend down to a maximum of 150 m, hyaloclastite formations dominate the stratigraphy to 1000 m and pillow basalt formations below 1200 m depth. Dike intrusions increase with increasing depth (Franzson, 2004). The highly permeable Holocene lavas and the uppermost part of the hyaloclastites (down to about 500 m) host a cold groundwater system and the overlying outflow of geothermal fluids (Franzson, 2004) except in the Gunnuhver area where hot fluids ascend toward the surface. The sediments below 400–500 m form a cap-rock for the geothermal system preventing the inflow of relatively cold saline ground water into the deeper part of the system. Most production wells receive fluid from aquifers of about 290 °C with the exception of RN-10 that produces from aquifers of about 315 °C (Björnsson et al., 2004). Resistivity anomalies coincide with the orientations and locations of the maximum intensity of the near surface alteration (Björnsson et al., 1971; Saemundsson et al., 2004), i.e., NE–SW consistent with the orientation of the nearby Stampar fissure swarm, and N–S consistent with the orientation of the less common right-lateral oblique-slip faults (Clifton and Schlische, 2003).

The areal extent of geothermal manifestations at Reykjanes is approximately 2 km^2 (Pálmason et al., 1985), but most of the current surface activity is concentrated in an area of approximately 0.2 km^2 (Fig. 1b). Surface geothermal manifestations at Reykjanes include steam vents, fractures emanating steam, steam heated mud pools, and warm ground (Fig. 1b). No boiling springs are currently present at Reykjanes, but a seawater geyser was active between 1906 and 1930 (Sapper, 1908; Bárdarson, 1931). Substantial silica sinter deposits further demonstrate past boiling spring activity at Reykjanes. The mode and intensity of surface geothermal activity at Reykjanes is known to change abruptly subsequent to seismic events in the region, such as in 1968, when a number of new steam vents appeared and previously calm mud pools started erupting (Jónsson, 1968). Similarly, in 1919 a new boiling spring appeared after a seismic event (Thorkelsson, 1928).

The steam vents and steam heated mud pools are located in the two most active and intensely altered parts of the geothermal area (Fig. 1b). The larger of the two, the Gunnuhver area, is located in the southeastern end of the area and is characterized by intensive steam vent activity and mud pools occur at the base of small hills. The smaller area is on the flats towards the northwestern end, near the shore of the spent brine pond. Mud pools are much more prevalent in that area and steam vents only occur on its margins. These two areas are for the most part unvegetated and the soil consists of wet, light colored clay, in places covered with hard crust.

The warm ground is mostly situated between the two areas of intense steam vent and mud pool activity (Fig. 1b). Large patches of warm ground also occur to the north and the south of the Gunnuhver steam vent area. The characteristic vegetation for the warm ground is bright green moss (*Hypnum jutlandicum*) and creeping thyme (*Thymus praecox arcticus*) (Elmarsdóttir et al., 2003). The soil is generally sandy clay and intermittently it is very densely packed under the vegetation cover.

The most active steam emanating fracture cuts across the eastern side of the steam vent area by Gunnuhver. Several other fractures that give off some steam are located in and around the area. Two N–S trending fractures are inferred from linear arrangement of steam emanations in the area between the two steam vent – mud pool areas. The steam from the fractures differs from that of the steam vents because it does not have the characteristic odor of H_2S.

3. Methods

3.1. Diffuse CO_2 flux through soil

Carbon dioxide flux through soil (φ_{CO_2}) was measured in a rectangular sampling grid that was laid out over the part of the area that showed significant surface activity (Fig. 1b). The length and width of the sampling grid were 600 and 375 m, respectively, and the grid spacing was 25 by 25 m. A total of 352 measurements were made in the grid as 48 points were located in the spent brine pond and were thus not accessible.

The CO_2 flux was measured directly using a closed-chamber CO_2 flux meter from West Systems equipped with a LICOR LI-820 single-path, dual wavelength, non-dispersive infrared gas analyzer.

All flux measurements were made using a chamber with 3.06×10^{-3} m^3 total internal volume and 3.14×10^{-2} m^2 basal area. The flux measurement is based on the rate of CO_2 increase in the chamber. Because φ_{CO_2} through the soil at Reykjanes was fairly moderate, the CO_2 concentration increase was generally linear for several minutes, allowing for relatively precise flux determinations.

The vegetation cover and the uppermost few centimeters of the soil were removed at least 1 h prior to flux measurements. The observed flux was generally high immediately after soil removal but decreased with time and reached a steady level within 30 min. The chamber was pressed firmly against the ground and loose soil was packed around the chamber on the outside. The CO_2 flux measurements were only conducted when dry weather conditions had prevailed for at least 2 days in order to avoid potential effects of water saturation of the soil pores (Granieri et al., 2003).

3.2. Heat flux through soil

The heat flux through the soil in the study area was estimated from soil temperature measurements using the method of Dawson (1964). This method, which was calibrated by direct measurements at the Wairakai thermal field, New Zealand, is based on correlation between soil temperature at 15 cm depth (t_{15}) and surface heat flux measured by a portable calorimeter. Where t_{15} was below 97 °C the heat flux through the soil (q_S in W/m^2) was estimated by:

$$q_S = 5.2 \times 10^{-6} t_{15}^4, \quad (1)$$

where t_{15} is in °C. If t_{15} was 97 °C or higher, the depth to the point where the soil temperature reaches that temperature (d_{97}; in cm) allows estimation of the heat flow through soil by:

$$q_S = 10^{((\log d_{97} - 3.548)/-0.84)}. \quad (2)$$

Eq. (2) is a best line fit through data from Dawson (1964) as reported by Gudmundsdóttir (1988). Gudmundsdóttir (1988) conducted measurements similar to those of Dawson (1964) at the Nesjavellir geothermal area Iceland. She used a portable calorimeter and soil temperature measurements and found that the empirical formulas of Dawson (1964) applied reasonably well to the relationship between heat flux and soil temperature in the geothermal soil at Nesjavellir. The temperature at 15 cm depth was measured at all points of the sampling grid, either in the footprint of the flux meter chamber or within 10 cm of it. The depth to 97 °C (d_{97}) was measured at eight points where t_{15} was 97 °C or higher. Individual point measurements of heat flux were used to determine the total heat flow through soil from the study area (H_S; in W). Assuming that heat flow through the soil is a manifestation of transport of steam from the geothermal reservoir to the surface, the mass flow of steam through the soil, F_{S,H_2O} in kg s^{-1}, can be computed as:

$$F_{S,H_2O} = \frac{H_S}{(h_{s,100°C} - h_{w,t_r})}, \quad (3)$$

where $h_{s,100\ °C}$ is the enthalpy of steam at 100 °C and h_{w,t_r} is the enthalpy of water at 5 °C, the average annual temperature at Reykjanes (2676 and 21 kJ kg^{-1}, respectively; Schmidt and Grigull, 1979).

3.3. Steam flow and CO_2 emissions from steam vents

The steam and heat flow from steam vents and fractures was determined by measuring or estimating the mass flow rate of steam (F_{V,H_2O}; kg s^{-1}) from individual vents and fractures shown in Fig. 1b. Steam flow rate from individual vents was measured by funneling the steam into a pipe of known radius where a Kurz model 2445 hot wire anemometer probe was located. The diameter of the measuring pipe was either 11 or 15 cm depending on the steam flow rate. The measuring pipe was placed directly on top of the smaller vents, but for the larger vents and fractures it was necessary to use a cone shaped rubber–cloth tent to direct the steam into the pipe. The area that could be covered with the largest tent was about 2 by 4 m. Fig. 2 shows a steam velocity measurement being conducted using a small tent attached to an 11 cm diameter measuring pipe.

The mass flow rate of steam, F_{V,H_2O}, from individual steam vents and fractures was calculated by:

$$F_{V,H_2O} = \frac{Pvr^2\pi}{RT} MW_{H_2O}, \quad (4)$$

where P is the pressure of the steam, assumed to be equal to 1.013 bar, v the steam velocity in the pipe in m s^{-1}, r the radius of the pipe in m, R the universal gas constant (8.314×10^{-5} m^3 bar mol^{-1} K^{-1}), T the temperature in K, and MW_{H2O} is the mole weight of H_2O (0.018 kg mol^{-1}). The temperature was in all cases between 99 °C and 101 °C so T was taken to be equal to 373.15 K when F_{V,H_2O} was calculated for individual vents. The steam

Fig. 2. Measurement of steam mass flow using hot-wire anemometer.

velocity was measured at 1 cm intervals from the wall of the pipe to the center. The maximum difference between the steam velocity in the center and that by the walls was generally <20%; it was <10% for the larger vents where steam velocity was high. Consequently, in the calculations the average of all steam velocity readings for individual vents was used. Steam flow from the smaller vents and fractures was estimated by visually comparing the size of the smaller steam plumes to plumes from larger vents where the flow rate had been measured. The validity of this method was checked by estimating the steam flow rate from selected steam vents before they were measured. The estimates generally agreed reasonably well with measurements, although the difference was up to 30–50% in some cases. Because the estimated steam flow was only about 18% of the total flow (i.e., measured + estimated) it was assumed that the uncertainty that is introduced by using this method is considerably less than about 10% of the total steam flow. The heat flow from steam vents and steam emanating fractures (H_V; W) was calculated by

$$H_V = F_{V,H_2O} h_{s,100^\circ C}. \quad (5)$$

The CO_2 discharge from steam vents and steam emanating fractures (F_{V,CO_2}; g s^{-1}) is the product of the mass flow of steam from these sources and the CO_2 concentration in the steam:

$$F_{V,CO_2} = F_{V,H_2O} C_{CO_2}, \quad (6)$$

where C_{CO_2} is the concentration of CO_2 in the steam in g kg^{-1}. Representative CO_2 concentration for the geothermal steam at Reykjanes was defined by theoretical considerations that were checked against chemical analyses of steam from selected steam vents and fractures (see Section 3.5 below).

3.4. Heat flow and CO_2 emissions from steam heated pools

Methods described by Dawson (1964) and Sorey and Colvard (1994) were used to calculate the total heat loss from steam heated pools, H_P, as the sum of heat loss by evaporation (H_e), conduction and molecular diffusion (H_c), and radiation (H_r):

$$H_P = H_e + H_c + H_r. \quad (7)$$

The heat loss from a pool by evaporation is calculated by:

$$H_e = A(h_{s,t_P} - h_{w,t_P})(0.0065 + 0.0029w) \times \frac{P_{H_2O}, t_P - P_{H_2O,atm}}{P_{total}}, \quad (8)$$

where A is the surface area of the pool in m^2, h_{s,t_P} and h_{w,t_P} refer, respectively, to the enthalpy of steam and of water at the temperature of the pool (t_P) both in J kg^{-1}, w is wind speed in m s^{-1}, P_{H_2O,t_P} and $P_{H_2O,atm}$ are the vapor pressures of water at the temperature of the pool and the atmospheric vapor pressure, respectively, both in bar, and P_{total} is the

total pressure in bar. The heat loss by conduction and molecular diffusion, H_c, is related to H_e by the Bowen ratio, RB (Sutton, 1953):

$$\mathrm{RB} = \frac{H_c}{H_e} = 6.1 \times 10^{-4} P_{\mathrm{total}} \frac{(t_P - t_{\mathrm{atm}})}{(P_{\mathrm{H_2O},t_P} - P_{\mathrm{H_2O,atm}})}, \quad (9)$$

where t_{atm} is the atmospheric temperature in °C. Radiative heat loss, H_r, is calculated by:

$$H_r = A\varepsilon\sigma(T_P^4 - T_{\mathrm{atm}}^4), \quad (10)$$

where ε is emissivity, equal to 0.955 for water, σ is the Stefan–Boltzman constant equal to 5.68×10^{-8} W m^{-2} K^{-4}, and T_P and T_{atm} refer to the temperature of the pool and the ambient temperature, respectively, both in K.

The water temperature in the nine largest pools at Reykjanes (see Fig. 1) was measured on four occasions under different weather conditions. Water temperature was measured in the uppermost few cm in the pools with a calibrated digital thermometer. Wind speed and atmospheric temperature were measured by a Kurz 2445 hot wire anemometer. The atmospheric temperature was also measured with the digital thermometer and the readings of the two thermometers were consistent within 1 °C. The atmospheric vapor pressure was calculated both from relative air humidity measurements at Keflavík airport, which is located 20 km NNW of Reykjanes, and from the measured atmospheric temperature.

If the pool temperature is constant, the heat loss, H_P, must be equal to the total heat input and it is assumed that steam condensation is the only mechanism of heat transfer into the pools, i.e., they are not fed by hot water. Accordingly, the mass flow of steam into the pool, F_{P,H_2O}, in kg s^{-1} can be computed by:

$$F_{P,H_2O} = \frac{H_P}{(h_{s,100°C} - h_{w,t_P})}, \quad (11)$$

where $h_{s,100\ °C}$ is the enthalpy of steam at 100 °C, in J kg^{-1}. Gas bubbles are visible in all pools, indicating that pool water is saturated with respect to dissolved CO_2. Consequently, it can be assumed that the CO_2 entering the pool, together with the steam will be released to the atmosphere. Assuming that the CO_2 concentration in the steam entering the pools is equal to the representative CO_2 concentration of the area, C_{CO_2}, as discussed in Section 3.5 below, the CO_2 discharge from the steam heated pools, F_{P,CO_2}, can be computed by

$$F_{P,CO_2} = F_{P,H_2O} C_{CO_2}. \quad (12)$$

3.5. Theoretical estimation of the representative CO_2 concentration in steam at Reykjanes

A systematic correlation between aquifer temperature and CO_2 concentration in geothermal fluids is commonly observed in high-temperature geothermal systems (Nehring and D'Amore, 1984; D'Amore and Truesdell, 1985; Arnórsson and Gunnlaugsson, 1985; Zhao and Ármannsson, 1996; Stefánsson and Arnórsson, 2002). This indicates that the activity of dissolved CO_2 in the deep fluid is controlled by local equilibrium between the geothermal solution and secondary minerals, at least during times of moderate CO_2 input. These apparent equilibrium conditions can be temporarily disturbed by excessive CO_2 input as a result of magmatic intrusions into the roots of geothermal systems, as was observed in the Krafla geothermal system during the Krafla volcanic events between 1975 and 1984 (Ármannsson et al., 1989).

Arnórsson et al. (1998) and Stefánsson and Arnórsson (2002) proposed that the activity of dissolved CO_2 in geothermal solutions above 230 °C in Icelandic geothermal systems is controlled by equilibrium between epidote solid solution, calcite, quartz, and prehnite described by the reaction

$$\underset{\text{epidote}}{2Ca_2Al_3Si_3O_{12}(OH)} + \underset{\text{calcite}}{2CaCO_3} + \underset{\text{quartz}}{3SiO_2} + 2H_2O = \underset{\text{prehnite}}{3Ca_2Al_2Si_3O_{10}(OH)_2} + 2CO_{2,aq}. \quad (13)$$

Assuming that the activity of calcite, quartz, and water is equal to unity, the logarithm of the activity of dissolved CO_2, $a_{CO_{2,aq}}$, can be expressed as

$$\log a_{CO_{2,aq}} = 1/2 \log K + \log a_{czo} - 3/2 \log a_{pre}, \quad (14)$$

where a_{czo} and a_{pre} refer to the activity of the Fe-free epidote endmember (clinozoisite) and prehnite, respectively. Because CO_2 is an uncharged species, its activity can be taken to be equal to its molar concentration, as a first-order approximation.

The composition of epidote from the Reykjanes geothermal system, reported by Sveinbjörnsdóttir (1991) and Lonker et al. (1993), ranges between $X_{czo} = 0.34$ to -0.34 (X_{czo} is defined as $X_{czo} = \frac{Al-2}{Fe^{3+}+Al+Cr^{3+}-2}$; see Franz and Libscher, 2004). The median X_{czo} value of 38 analyses reported by

Sveinbjörnsdóttir (1991) and Lonker et al. (1993) is close to 0.17. Assuming ideal solid solution between clinozoisite and the epidote endmember in the epidote solid solution, the activity of clinozoisite is taken to be equal to the median X_{czo}, or 0.17. The only available data on prehnite composition from the Reykjanes system are three analyses reported by Lonker et al. (1993). The average of these analyses yields the mineral formula $Ca_2Fe_{0.2}Al_{1.8}SiO_{10}(OH)_2$. Assuming that Al–Fe substitution only takes place on the six-coordinated site and ideal solid solution between $Ca_2FeAlSi_3O_{10}(OH)_2$ and $Ca_2Al_2Si_3O_{10}(OH)_2$, the activity of the Fe-free endmember can be taken to be equal to the mole fraction of Al on the six-coordinated site or 0.8.

Fig. 3 depicts aqueous CO_2 concentrations in equilibrium with the mineral assemblage defined by reaction (13). The dashed curve shows the concentration of dissolved CO_2 in equilibrium with pure clinozoisite and prehnite (unit activity of both phases) and the solid curve represents equilibrium with a_{czo} equal to 0.17 and a_{pre} equal to 0.8. The value of the equilibrium constant for reaction (13), as a function of temperature along the liquid–vapor saturation curve for pure water, was calculated with the aid of the SUPCRT92 code (Johnson et al., 1992) using the accompanying *dprons92* database. Symbols indicate CO_2 concentrations in deep fluids from 4 wells at Reykjanes, RN-8, RN-9, RN-10, and RN-11 and three selected wells from the Svartsengi geothermal area, SV-8, SV-9, and SV-11. The deep fluid composition and aqueous speciation was computed by the program WATCH (Arnórsson et al., 1982) version *wdens23* (J.Ö. Bjarnason, personal communication). The reservoir temperatures, computed for each sample from the observed concentration of aqueous silica assuming equilibrium between the geothermal fluid and quartz, were consistent with measured temperatures in the wells. Inspection of Fig. 3 shows that observed CO_2 concentrations of the geothermal fluid at Reykjanes are in excellent agreement with predicted concentrations based on equilibrium for reaction (13) and the mineral compositions discussed above.

The concentration of CO_2 in the deep fluid at 290 °C, buffered by reaction (13) and assuming the mineral compositions described above, computed by Eq. (14) is equal to 1250 ppm. The steam fraction produced by adiabatic boiling from 290 °C to 100 °C is equal to 0.386 and assuming that the dissolved CO_2 will partition more or less quantitatively into the steam phase the composition of geothermal steam at the surface at Reykjanes, C_{CO_2}, will be equal to 3242 ppm CO_2 or about 3.2 g of CO_2 per kg of steam. In order to test this theoretical result, the CO_2 concentration in steam was measured from selected steam vents collected for this study and one of the steam emanating fractures. The steam sam-

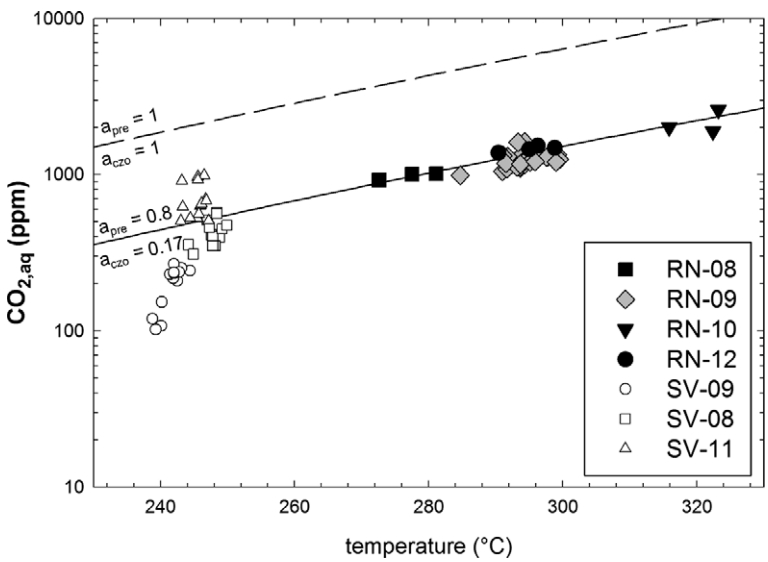

Fig. 3. Concentration of dissolved CO_2 in Reykjanes geothermal fluids. The curves represent computed CO_2 concentrations assuming equilibrium between the fluid, quartz, calcite, clinozoisite, and prehnite. The dashed curve represents unit activity for all phases but the solid curve is computed for clinozoisite and prehnite activities equal to 0.17 and 0.80, respectively. Filled symbols represent fluid compositions observed in geothermal wells at Reykjanes and open symbols in wells in the Svartsengi geothermal area.

ples were collected into evacuated Giggenbach bottles containing approximately 50 g of concentrated (50 wt%) NaOH solution. The concentrations of the NaOH soluble gases, CO_2 and H_2S, were analyzed by titration, whereas the other significant gases, N_2, Ar, O_2, H_2, and CH_4, were analyzed by gas chromatography. The observed CO_2 concentrations ranged between 3.2 and 20 g kg^{-1}. Eight gas analyses from Arnórsson and Gunnlaugsson (1985) showed an even wider range of CO_2 concentrations, that is from 3.7 to 32 g kg^{-1}. The lowest CO_2 concentrations observed in this study are from the largest steam vent and the largest fracture, together comprising more than 50% of the total steam flow from the area. Similarly, the lowest CO_2 concentrations reported by Arnórsson and Gunnlaugsson (1985) are from vents in the area of most intense steam discharge and the CO_2 concentrations were found to increase with increasing distance from the most active area. This indicates that the CO_2 concentration in uncondensed or primary steam from the geothermal reservoir is equal or very close to 3.2 g kg^{-1}, as predicted from Eq. (14), and that the higher gas concentrations, that were observed around the margins of the major steam up-flow zone, result from partial steam condensation.

4. Results

4.1. Soil diffuse degassing

The GSA method (Chiodini et al., 1998) permits the partition of complex distributions into different normal (or log-normal) populations and the estimation of the proportion (f_i), the mean (M_i), and the standard deviation (σ_i) of population i following the graphical procedure of Sinclair (1974), which is based on a detailed analysis of the distributions in probability plots. This method has been successfully applied to the results of CO_2 flux campaigns in order to both separate background populations from anomalous CO_2 flux populations (i.e., where the fluxes originate in deep volcanic-hydrothermal CO_2) and to compute the total CO_2 output, and relative uncertainties, from the different sources active in surveyed areas. The probability graph of log φ_{CO_2} in the Reykjanes thermal area (Fig. 4) shows that the entire data set fits a curve with two inflection points, compatible with the combination of three

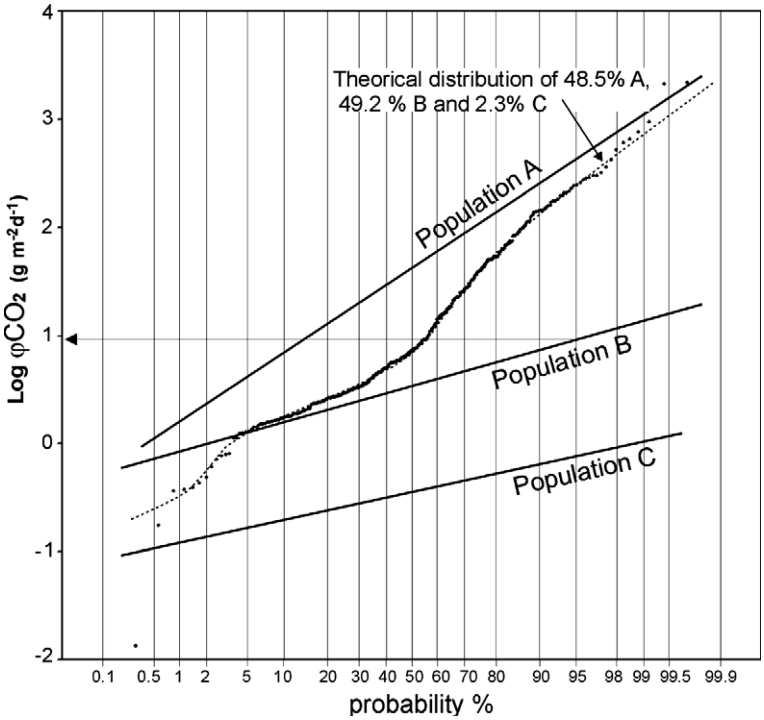

Fig. 4. Logarithmic probability plot of CO_2 flux through soil at Reykjanes. Three statistically distinct populations, A, B, and C, are present in the data set. Population A represents CO_2 flux of geothermal origin whereas B and C represent the background CO_2 flux from the soil in the area.

Table 1
Estimated parameters of the partitioned populations and diffuse CO_2 output (GSA method)

Population	f_i (%)	$M_i \pm \sigma_i$	MN_i (g m^{-2} d^{-1})	No. of points	S_i (m^2)	Source	F_{CO_2} (t d^{-1})
A	48.5	1.62 ± 0.61	112 (159–85)	171	106,875	Hydrothermal	12.0 (17.0–9.1)
B	49.2	0.53 ± 0.26	4.1 (4.4–3.7)	173	108,125	Background	0.44 (0.48–0.40)
C	2.4	-0.45 ± 0.20	0.4 (0.7–0.3)	8	5000	Background	0.0020 (0.0035–0.0015)
Total	**100**			**352**	**220,000**		12.4 (17.5–9.5)

Ninety-five percent confidence interval of the estimations is given in parenthesis.

theoretical populations with log normal distributions, A, B, and C in the proportions of 48.5%, 49.2%, and 2.3%, respectively.

The estimated f_i, M_i, and σ_i values for populations A, B, and C are reported in Table 1. Even if complete partitioning of the data is not possible because of partial overlapping of the populations, it is evident from Fig. 4 that $\log \varphi_{CO_2}$ values higher than 1 (i.e., φ_{CO_2} higher than 10 g m^{-2} d^{-1}) are mainly derived from population A, because less than 5% of the computed population B (and C) should have such high values (Fig. 4). Below the selected threshold, most of the φ_{CO_2} values are from populations B and C and only a small number are from population A. The frequency distribution of soil temperatures at 15 cm depth was used in order to better assess the sources of CO_2 (Fig. 5). The temperature of the soil in sites with low φ_{CO_2} (<10 g m^{-2} d^{-1}) values show an evident peak at values between 10 °C and 24 °C, which correspond to the background for the area. Conversely, for high φ_{CO_2} values (>10 g m^{-2} d^{-1}) soil temperatures range from background temperature to 100 °C. This finding clearly indicates that population A represents the hydrothermal source, while populations B and C are from background sources.

At Reykjanes, as well as in every studied area in the world, CO_2 flux values show a frequency distribution caused by partial overlapping of background and anomalous log-normal populations. Because the computed statistical parameters (i.e., M_i and σ_i) refer to the logarithm of values, the mean value of CO_2 flux (MN_i) and the central 90% confidence interval of the mean, listed in Table 1, are estimated by means of the Sichel's t-estimator (David, 1977).

The estimated mean flux values have been used to compute the total CO_2 output associated with each population (Table 1). An evaluation of the area covered by each population (S_i) is obtained by multiplying the study area ($S = 220{,}000$ m^2) by the corresponding proportion of the population (i.e., $S_i = f_i S$). The total CO_2 output associated with each population is then estimated by multiplying S_i by MN_i. The total CO_2 release from the entire study area can be obtained by summing the contribution of each population. Similarly, the central 90% confidence interval of the mean is used to calculate the uncertainty of the total CO_2 output estimation of each population. It can be seen from Table 1 that the total daily CO_2 output from the area surveyed (F_{S,CO_2}) is equal to 12.4 t d^{-1} (with 9.5 and 17.5 t d^{-1} as the maximum and minimum values, respectively, estimated from the σ_i-s of the three populations), of which 97% come from population A, i.e., of geothermal origin.

In a recent study Cardellini et al. (2003) used sequential Gaussian simulations (sGs) to analyze φ_{CO_2} data from several field campaigns. In this method, the sample set is used to generate a great number of equiprobable representations, or realizations of the spatial distribution of φ_{CO_2}. The advantage of using sGs is that this method results in more realistic values for uncertainties in the total flux than the GSA method, which tends to overestimate the uncertainty of MN_i for individual populations (Cardellini et al., 2003). 300 sequential Gaussian simulations were performed using the sGs algorithm of the *sgsim* code by Deutsch and Journel (1998). The simulation domain was divided into 57,216 (198 by 298) square cells, each having a surface of 4 m^2. After the normal score transforming of the original data, an exponential variogram model of the normal scores (with nugget = 0.26, sill 1 and range 130 m) that fits the experimental values for distances shorter than the range was used (Fig. 6).

The results of the 300 simulations are depicted in Fig. 7a that shows the mean φ_{CO_2} of individual cells in the model. Fig. 7b shows the results of the 300 simulations in terms of the total mass flow of CO_2 through the soil resulting from each simulation. The mean F_{S,CO_2} of the 300 simulations (13.5 t d^{-1}) is very similar to that obtained by the GSA method, but the standard deviation is smaller

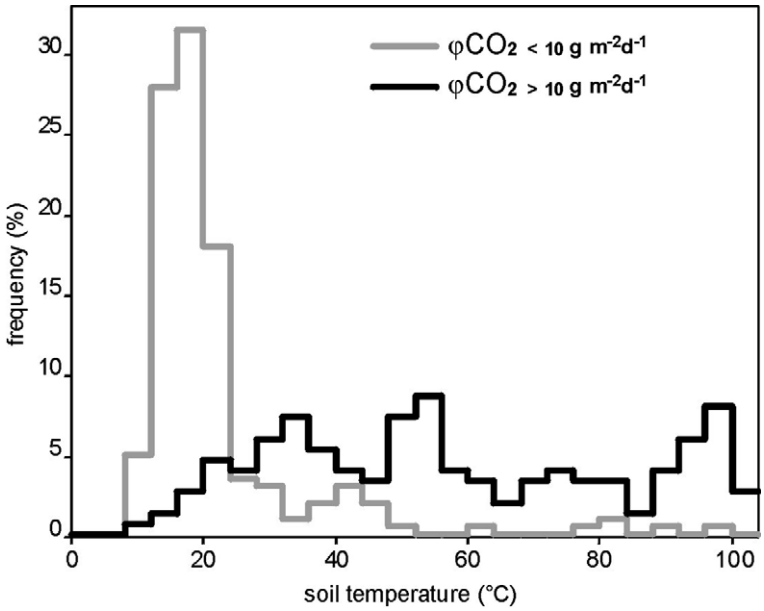

Fig. 5. A histogram showing soil temperatures at 15 cm depth for low φ CO_2 populations (<10 g m^{-2} d^{-1}) and for high φCO_2 populations (>10 g m^{-2} d^{-1}).

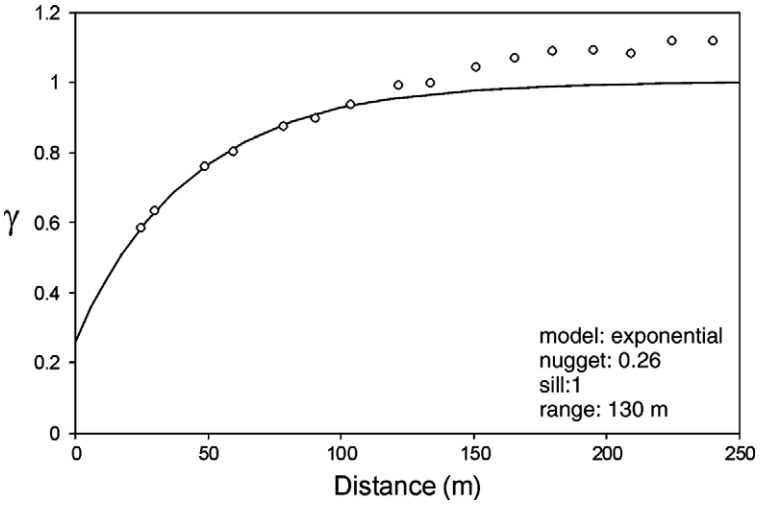

Fig. 6. Experimental semivariogram for φCO_2 measurements at Reykjanes.

(1.7 t d^{-1}). Assuming that CO_2 is transported toward the surface by steam with CO_2 concentration equal to the representative CO_2 concentration at Reykjanes (3.2 g kg^{-1}) we find that the amount of steam associated with the computed CO_2 flux must be equal to 4200 ± 530 t d^{-1}, which corresponds to 130 ± 16 MW of thermal energy (Eq. (5)). The F_{S,CO_2} values determined by the GSA and the sGs methods are in good agreement and for the purpose of the discussions below the F_{S,CO_2} value determined by the sGs method will be used.

4.2. Heat flow through soil

The heat flux through soil at Reykjanes computed using Eqs. (1) and (2) ranged from 0.04 to 3000 W m^{-2} and the average value of all 352 measurements was equal to 77.6 W m^{-2}. Sequential

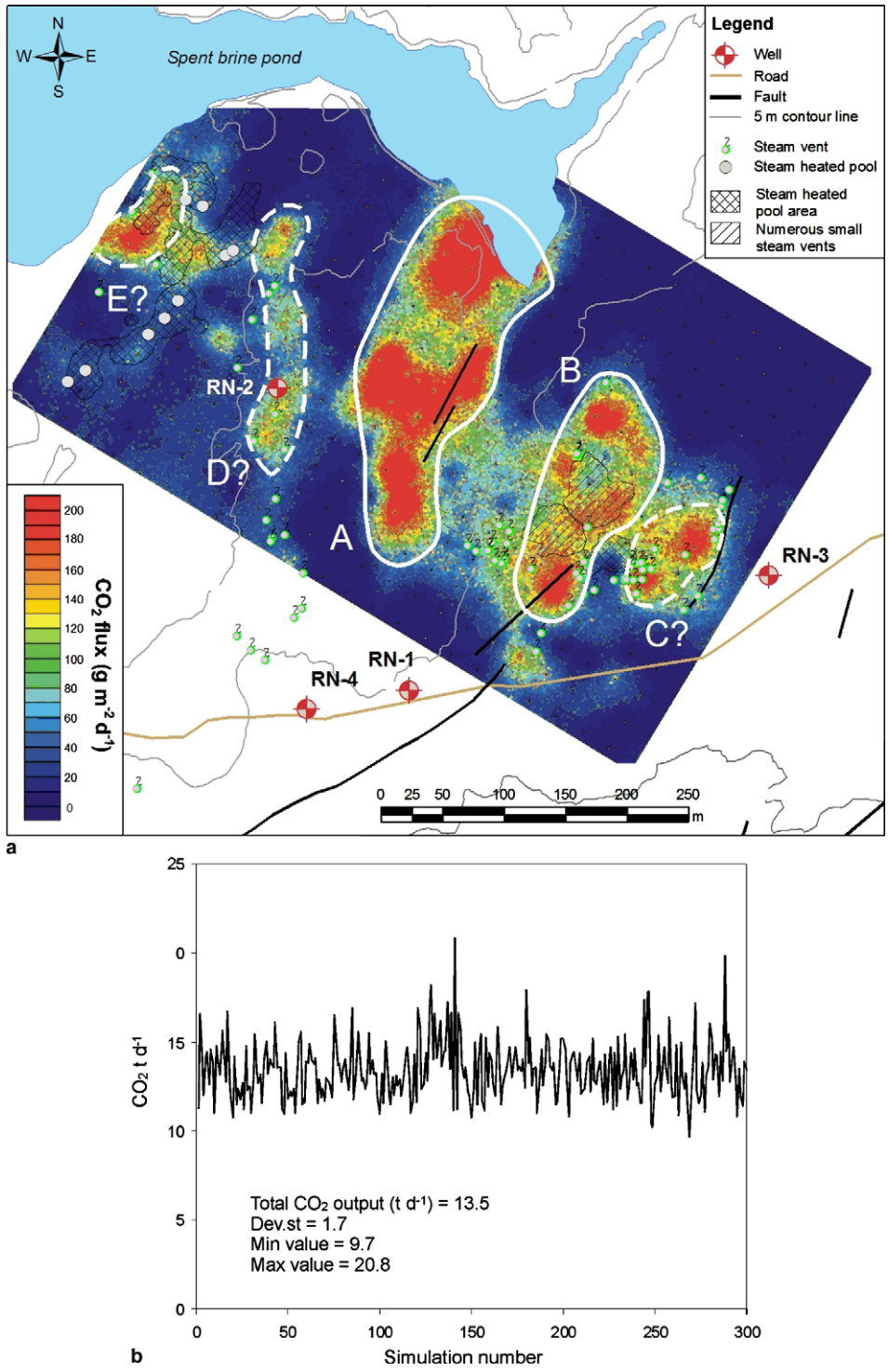

Fig. 7. Results of sequential Gaussian simulations of diffuse CO_2 flux through the soil at Reykjanes. (a) Map showing the mean φ CO_2 individual model cells. Labels A through E indicate possible diffuse degassing structures (marked with question marks and dashed boundaries when uncertain). (b) Model results for total mass flow of CO_2 through the soil at Reykjanes for the 300 individual simulations.

Gaussian simulations were used to evaluate the total heat flow from the surveyed area, following more or less the same procedure as for the CO_2 flux data. Three hundred sGs's were performed and the simulated cells were 4 m^2. The heat flux data were normal scored and a spherical variogram model (with nugget = 0.21, sill 1 and range 190 m) was used to fit the experimental variogram. The results of the 300 simulations are depicted in Fig. 8 showing the mean heat flow of individual cells in the model. The average heat flow value of 300 realizations was 16.9 MW from the study area and the standard deviation was equal to 1.4 MW. This value is in good agreement with the results of Björnsson et al. (1971) who reported heat flow through surface as 17.4 MW from the whole geothermal area at Reykjanes. Assuming that condensation of ascending steam is the dominating heat transport mechanism, the corresponding mass flow of steam through the soil at Reykjanes computed using Eq. (3) is equal to 550 t d^{-1}. Note that the heat flow value obtained by soil temperature measurements is much smaller than the heat flow inferred from the observed F_{S,CO_2} and the estimated primary steam composition (see Section 4.1).

4.3. Steam and CO_2 discharge from steam vents and fumaroles

A total of 52 steam vents and 33 steam emanating fractures were identified in the study area, most of which were located within the area defined by the sampling grid of the soil diffuse degassing measurements. The steam flow was measured directly from 25 of the steam vents and two of the fractures and estimated from the remaining 58 vents and fractures. As noted above, the steam discharged from the measured vents and fractures amounted to

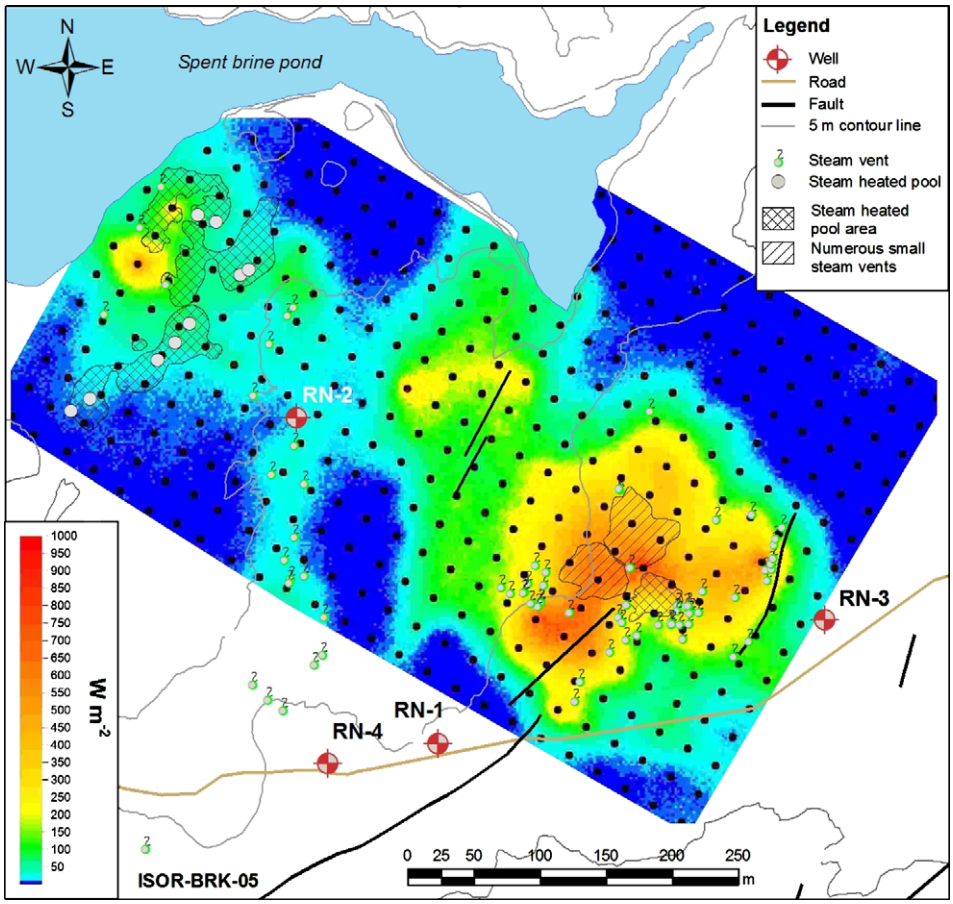

Fig. 8. Results of sequential Gaussian simulations of heat flow through the soil at Reykjanes. The map shows the mean heat flow through individual model cells.

82% of the total steam discharge (measured and estimated).

The total mass flow of steam from steam vents and steam emanating fractures at Reykjanes, F_{V,H_2O}, was found to be equal to 0.82 ± 0.16 kg s^{-1}, or 71 ± 14 t d^{-1}. Of this about 80% were emitted through steam vents and the remaining 20% through the fractures. The estimated total uncertainty of this value, accounting for the uncertainty of the visual estimations and the uncertainty of the gas flow measurements is taken to be approximately ±20%. Accordingly, H_V is equal to 2.2 ± 0.4 MW. The corresponding value for total CO_2 discharge from steam vents and steam emanating fractures computed using Eq. (6) and taking C_{CO_2} to be equal to 3.2 g kg^{-1} is equal to 0.23 ± 0.05 t d^{-1}.

4.4. Heat flow and CO_2 discharge from steam heated pools

Water temperature was measured four times in the nine biggest steam heated pools at Reykjanes under different environmental conditions (i.e., atmospheric temperature, atmospheric vapor pressure, and wind speed). The total surface area of the pools is 84 m^2 ± 10% and measured water temperatures ranged from 26.6 °C to 92.6 °C. Measured surface temperatures of individual pools varied by as much as 28 °C between measurements as a result of variable weather conditions, particularly wind speed. The resulting heat flow from the steam heated pools, computed by Eqs. (8)–(10), ranged between 1.1 and 1.3 MW, with an average of 1.2 ± 0.1 MW. The total heat loss from the pools as well as the weather conditions during the pool measurements are reported in Table 2. The corresponding mass flow of steam computed by Eq. (11) is 0.45 ± 0.08 kg s^{-1} or 39 ± 7 t d^{-1}. The corresponding value for the mass flow of CO_2 from the pools is 1.45 ± 0.4 g s^{-1} or 0.125 ± 0.03 t d^{-1}. The resulting values for F_{CO_2}, F_{H_2O}, and H through soil, steam vents and fractures, and steam heated pools at Reykjanes are summarized in Table 3.

Table 2
Total heat loss from steam heated pools (H_P) and environmental conditions during measurement

Date	Atmospheric temperature (°C)	Atmospheric vapor pressure (mbar)	Wind speed (m s^{-1})	H^P_{total} (MW)
11 04 2004	4.8	6	6	1.3
12 13 2004	2.9	7	14	1.3
12 14 2004	−1.3	5	3.5	1.1
12 23 2004	−11.8	2	3.2	1.1

Table 3
Summary of results of F_{CO_2}, F_{H_2O}, and H through soil, steam vents and fractures, and steam heated pools at Reykjanes

	F_{CO_2} (t d^{-1})	F_{H_2O} (t d^{-1})	H (MW)
Soil	13.5 ± 1.7	4200 ± 530[a]/ 550 ± 46[b]	130 ± 16[a]/ 16.9 ± 1.4[b]
Vents/fractures	0.23 ± 0.05	71 ± 14	2.2 ± 0.4
Pools	0.125 ± 0.03	34.5 ± 7	1.2 ± 0.1

[a] Steam flow and heat flow inferred from observed CO_2 flux and CO_2 concentration in steam.
[b] Steam flow and heat flow based on measured soil temperatures.

5. Discussion

5.1. Total discharge of CO_2 to the atmosphere at Reykjanes

Natural atmospheric emissions of CO_2 at Reykjanes take place via three general pathways; soil diffuse degassing, steam vent discharge; and gas bubbling through steam heated pools. The combined CO_2 emission via these three pathways at Reykjanes is equal to 13.9 t d^{-1} or 5060 metric tons a^{-1}. Most of this CO_2, by far (97.4%), is emitted through soil diffuse degassing, while only 1.7% and 0.9% are emitted through steam vents and fractures and steam heated pools, respectively. It must be noted that the CO_2 flux by soil diffuse degassing was determined directly, whereas the CO_2 emissions from steam vents and steam heated pools were determined by indirect methods. The most likely source of error in the estimations of CO_2 emissions from steam vents and steam heated pools is that the representative CO_2 concentration in steam in the area may be underestimated. However, even if the representative CO_2 concentration in steam is grossly underestimated by a factor of 4 the soil diffuse degassing, nevertheless, accounts for more than 85% of the total natural CO_2 emissions from the Reykjanes geothermal area. As noted above, the Reykjanes volcanic system has been dormant during the last 800 a or so, whereas geologic evidence indicates that episodes of volcanic activity occur with about 1000 a intervals (Sigurgeirsson, 2004). The relatively long repose period since the last volcanic episode at Reykjanes suggests that the present rate of CO_2 degassing may be at a minimum and it may have

been significantly higher immediately after volcanic episodes with associated dike intrusions.

Despite a large number of recent studies of natural CO_2 emissions from geothermal systems, the relative proportions of diffuse to focused emissions have generally not been determined. The two notable exceptions, Favara et al. (2001) and Werner et al. (2000), indicate that soil diffuse degassing is generally a major, if not the dominating pathway of CO_2 release from geothermal systems, as appears to be the case at Reykjanes. Favara et al. (2001) found that soil degassing (both diffuse and focused) accounted for 96% of the CO_2 emissions from soil, steam vents, and bubbling through surface waters at Pantelleria Island volcano, Italy. Werner et al. (2000) reported that focused degassing amounted to 32–63% of the total CO_2 emissions at Mud Volcano in Yellowstone, USA. Later, Werner and Brantley (2003) suggested that the proportion of vent emissions at Mud Volcano was likely higher than in other parts of the Yellowstone system.

Ármannsson et al. (2005) estimated that the maximum CO_2 emissions from all Icelandic geothermal systems were 1.3×10^6 t a^{-1} based on geological observations. Earlier estimates of total CO_2 discharge from Icelandic geothermal systems range between 0.15×10^6 t a^{-1} (Ármannsson, 1991) and $1–2 \times 10^6$ t a^{-1} (Arnórsson, 1991; Arnórsson and Gíslason, 1994; Óskarsson, 1996). The lower value refers to steam vent discharge only, whereas the higher values represent the estimated total release of CO_2 from Icelandic geothermal systems, including atmospheric emissions (via soil diffuse degassing, steam vents, and steam heated pools), as well as CO_2 discharge into groundwater. Ármannsson et al. (2005) suggested that the discrepancy between the estimates might be due to their different nature, i.e., that the vent emissions constitute only a small fraction of the total emissions. The results of the present study, therefore, support this interpretation. The total CO_2 emissions from Reykjanes are also in qualitative agreement with the estimates of total CO_2 emissions from Iceland, when normalized to aerial extent of high-temperature geothermal activity. The areal extent of geothermal activity at Reykjanes is about 2 km^2 or only 0.3% of all geothermal systems in Iceland (total areal extent is 600 km^2; Pálmason et al., 1985). If it is assumed that all of the CO_2 emission at Reykjanes occurs in the study area and the observed emissions normalized to the 2 km^2 of surface manifestations at Reykjanes, the CO_2 emissions per unit surface area at Reykjanes are found to be 2500 t a^{-1} km^{-2}. If this value is representative for all other geothermal areas in Iceland the total emissions from the country would be equal to 1.5×10^6 t a^{-1}. This good agreement with previous estimates, although probably partly fortuitous, indicates that the above estimates for total natural CO_2 emissions from Iceland are, at least, of the right order of magnitude.

5.2. Geologic controls of CO_2 emissions at Reykjanes

The spatial distribution of soil diffuse degassing (Fig. 7a), soil temperature (Fig. 1b) and heat flow (Fig. 8) indicates a strong tectonic control of both diffuse CO_2 emissions and heat loss. Figs. 1b, 7a, and 8, illustrate two well-defined linear diffuse degassing and heat loss structures, labeled A and B in Fig. 7a (referred to hereafter only as diffuse degassing structures; DDS), that are semiparallel to each other; DDS A is located approximately in the center of the study area and DDS B about 100 m to the SE of DDS A. In addition to these bigger DDSs, two or possibly three smaller linear features can be seen (labeled C, D, and E in Fig. 7a). The orientation of the DDSs is in all cases between N–S and NNE–SSW (between 000° and 020°). It can also be seen from the figures that the most active parts of the DDSs define a NW–SE trend.

Clifton and Schlische (2003) made an extensive study of fracture- and fault-orientation at Reykjanes and in other volcanic systems on the Reykjanes peninsula. They found that fracture orientation was a function of location with respect to the center of the zone of active volcanism. They reported that, in general, fractures tend to be more northerly trending near the center of the rift zone than at its margins (i.e., the mean strike of fractures was 037° around Grindarvík compared to 051° in the Vogar region). They also reported that the vast majority of the fractures in the Reykjanes area were normal faults or extensional fractures, but they also described a few N–S trending right lateral strike-slip faults confined to the center of the rift zone, such as at Reykjanes. The orientation of the DDSs in the Reykjanes geothermal area is consistent with the orientation of the right lateral strike-slip faults reported by Clifton and Schlische (2003).

Comparison between the spatial distribution of diffuse degassing (Fig. 7a) and heat flow (Fig. 8), illustrates that elevated heat flow through soil generally coincides with DDSs. However, from a closer inspection, it is apparent that the most prominent

DDS (A) has only relatively moderate heat flow through soil compared to the second biggest one (B). These two DDSs are also characterized by different soil types; DDS A occurs in moss covered, brownish and relatively unaltered sandy/clay rich soil, whereas DDS B is characterized by unvegetated, light-colored, wet geothermal clay, indicative of extensive geothermal alteration. The authors suggest that the different CO_2-emission/soil-temperature ratio of these two DDSs is a result of extensive steam condensation under DDS A, whereas very little condensation seems to occur under DDS B.

This interpretation is supported by the large discrepancy between the observed heat flow through the surface at Reykjanes, 16.9 MW, and the thermal energy released by condensing the 4200 t d^{-1} of steam that must be associated with the observed CO_2 flux to the atmosphere, which is equal to 130 MW. The difference between these values is most probably a result of condensation of a large fraction of the steam (at least 87%) in the subsurface. The thermal energy from steam condensation at depth is likely transported laterally out of the system by groundwater flow. A portion of the ascending CO_2 must also be dissolved in the groundwater. However, uncertainties about the groundwater flow velocity, the thickness of the groundwater body and the areal extent of the zone where steam and groundwater interact, prevent quantification of the amount of CO_2 that is dissolved in groundwater and transported away from the geothermal area in the subsurface. The observed CO_2 emissions from the Reykjanes geothermal area must thus be taken to represent a minimum value for the release of CO_2 from the geothermal reservoir. The heat loss inferred from the observed CO_2 release, 130 MW, similarly represents a minimum value for the natural heat loss of the Reykjanes geothermal reservoir.

The substantial interactions between groundwater and ascending geothermal steam, indicated by the results of this study, are consistent with observed hydrothermal alteration, temperature profiles in drill holes, and recent TEM-resistivity measurements. Elevated hydrothermal alteration is observed at shallow levels above the cold groundwater layer (Franzson et al., 2002; Franzson, 2004). Temperature profiles from drill holes indicate the presence of a shallow groundwater current, in permeable Holocene lavas, flowing toward the SW through the present study area (A. Hjartarson, personal communication). Furthermore, recent TEM resistivity measurements indicate the presence of a thin low-resistivity horizon near the surface at Reykjanes that has been interpreted as a cold and saline groundwater aquifer (Karlsdóttir, 2005). Very high permeability of the bedrock in this area is evidenced by tidal wave variations in the water level in drill hole RN-05 that are about 33% of the oceanic tidal wave (Björnsson et al., 1971). The extent and modes of surface geothermal manifestations at Reykjanes are probably sensitive to relatively small changes in the hydrological conditions in the groundwater aquifer. Although such changes are not likely to affect the rate of CO_2 release from the deep geothermal reservoir, they can change the relative proportions between discharge of CO_2 into the atmosphere and that into groundwater. Interactions between surface geothermal activity and groundwater will, therefore, tend to amplify temporal variability of surface geothermal activity and thus atmospheric CO_2 discharge from the Reykjanes geothermal system.

5.3. Environmental impact of a 100 MWe power plant at Reykjanes

One of the objectives of this study was to quantify the natural CO_2 emissions from the Reykjanes geothermal system prior to the installation of a 100 MWe power plant, commissioned in May 2006. Until that time the production was limited to one drillhole and several new wells that have been discharged temporarily for flow tests. Emission measurements under the current low-production conditions allow for the evaluation of possible changes in natural CO_2 emissions as a result of extensive production in the near future and the evaluation of the environmental impact of geothermal power production by providing a reference value of natural emissions to compare with the CO_2 emissions from the proposed power plant.

Three major geothermal power plants are currently operated in Iceland, at Nesjavellir and Svartsengi in the SW and at Krafla in the NE. Natural CO_2 emissions from Reykjanes determined in this study are significant compared to the release from the Nesjavellir power plant (62 MWe), where 13,200 tons of CO_2 were released in 2000. However, the natural emissions from Reykjanes are very small compared to the release from the Svartsengi (45 MWe) and Krafla (60 MWe) geothermal power plants (each released about 75,000 metric tons of CO_2 in 2000). The relatively high CO_2 emissions

from Svartsengi are a result of a shallow steam cap that formed in the northeastern part of the geothermal system after a few years of production (see Ármannsson et al., 2005). The concentration of CO_2 is much higher in the steam cap than in steam from the liquid dominated parts of the system, and production from the steam cap has caused a dramatic increase in the CO_2 emissions from the power plant. On the other hand, the high CO_2 emissions from Krafla have been attributed to a pulse of magmatic CO_2 into the geothermal reservoir during the volcanic activity in the period from 1975 to 1984, generally referred to as the Krafla fires (see Ármannsson et al., 2005).

Production of 100 MWe at Reykjanes requires approximately 168 kg s^{-1} of steam (S. Thórhallsson, personal communication). The steam will be separated at a pressure of 19 bar-a; taking 290 °C as the reservoir temperature, the corresponding steam fraction under these conditions will be 0.207. If the concentration of CO_2 in the deep fluid is taken to be equal to 1250 ppm (see Section 3.5) and the CO_2 is assumed to partition quantitatively into the steam, the concentration of CO_2 in the steam will be approximately 6000 ppm or 0.6% of the steam mass flow. The resulting emissions of CO_2 from the planned power plant will be approximately 1 kg s^{-1} or 31,600 t a^{-1}. This value is a minimum estimate, because if a significant portion of the production at Reykjanes will be from wells that produce from the hottest parts of the geothermal reservoir, e.g., well RN-10, the CO_2 concentration of the produced steam could be significantly higher than 0.6%. Note that these calculations assume neither that production will result in the formation of a steam cap in the geothermal system nor that magmatic activity may increase the concentration of CO_2 in the deep fluid as happened in Krafla.

The above calculations demonstrate that the planned power plant at Reykjanes will significantly increase the CO_2 emissions from the geothermal system. If the present natural emissions do not change with time in response to production the increase will be about sixfold.

Acknowledgements

We thank I. Thorbergsdóttir for her help with the preparation of this project. R.F. Reynisson, G.B. Ingvarsson, and M. Ólafsson helped with field work at Reykjanes. E. Ilyinskaya and A.Í. Thórhallsson helped with the preparation of this manuscript. S. Thordarson helped with data processing. Discussions and email correspondence with C. Cardinelli, Á. Ragnarsson, M. Sorey, G. Gíslason, S. Arnórsson, H. Franzson, and K. Saemundsson were very helpful. Funding for this project was provided by The Icelandic Research Center (Rannís), Icelandic National Energy Authority, The National Power Company, Sudurnes Regional Heating Corp., and Iceland GeoSurvey.

References

Ágústsdóttir, A.M., Brantley, S.L., 1994. Volatile fluxes integrated over 4 decades at Grímsvötn volcano, Iceland. J. Geophys. Res. 99 B5, 9505–9522.

Aiuppa, A., Caleca, A., Federico, C., Gurrieri, S., Valenza, M., 2004. Diffuse degassing of carbon dioxide at Somma–Vesuvius volcanic complex (Southern Italy) and its relation with regional tectonics. J. Volcanol. Geotherm. Res. 133, 55–79.

Allard, P., Carbonelle, J., Dajlevic, D., Le Bronec, J., Morel, P., Robe, M.C., Maurenas, J.M., Faivre-Pierret, R., Martin, D., Sabroux, J.C., Zettwoog, P., 1991. Eruptive and diffuse emissions of CO_2 from Mount Etna. Nature 351, 387–391.

Ármannsson, H., 1991 Geothermal energy and the environment. In: Geoscience Society of Iceland. Conf. Geology and Environmental Matters. Prog. and Abstr., pp. 16–17 (In Icelandic).

Ármannsson, H., Benjamínsson, J., Jeffrey, A., 1989. Gas changes in the Krafla geothermal system, Iceland. Chem. Geol. 76, 175–196.

Ármannsson, H., Fridriksson, Th., Kristjánsson, B.R., 2005. CO_2 emissions from geothermal power plants and natural geothermal activity in Iceland. Geothermics 34, 286–296.

Arnórsson, S., 1991. Estimate of natural CO_2 and H_2S flow from Icelandic high-temperature geothermal areas. In: Conf. Geology and Environmental Matters. Prog. and Abstr., pp. 18–19 (In Icelandic).

Arnórsson, S., Gíslason, S.R., 1994. CO_2 from magmatic sources in Iceland. Miner. Mag. 58A, 27–28.

Arnórsson, S., Gunnlaugsson, E., 1985. New gas geothermometers for geothermal exploration – calibration and application. Geochim. Cosmochim. Acta 49, 1307–1325.

Arnórsson, S., Fridriksson, Th., Gunnarsson, I., 1998. Gas chemistry of the Krafla Geothermal field, Iceland. In: Arehart G.B., Hulston J.R. (Eds)., Proceedings of the 9th International Symposium Water–Rock Interaction, WRI-9, pp. 613–616.

Arnórsson, S, Sigurdsson, S., Svavarsson, H., 1982. The chemistry of geothermal waters in Iceland 1. Calculation of aqueous speciation from 0 °C to 370 °C. Geochim. Cosmochim. Acta 46, 1513–1532.

Bárdarson, G.G., 1931. The warm sea water pool at Reykjanes. Náttúrufreadingurinn 1, 78–80 (in Icelandic).

Baubron, J.C., Allard, P., Toutain, J.P., 1991. Diffuse volcanic emissions of carbon dioxide from Vulcano Island, Italy. Nature 344, 51–53.

Björnsson, S., Ólafsdóttir B., Tómasson J., Jónsson J., Arnórsson, S., Sigurmundsson, S.G., 1971. Reykjanes. Final report on investigations in the geothermal area. National Energy Authority report (in Icelandic).

Björnsson, G., Ólafsson, M., Jónasson, H., Magnússon, Th. M., 2004. Production studies of wells RN-9, RN-10, RN-11 and RN-12 in Reykjanes (2002–2004). Iceland GeoSurvey report ÍSOR-2004/019 (in Icelandic).

Brombach, T., Hunziker, J.C, Chiodini, G., Cardellini, C., Marini, L., 2001. Soil diffuse degassing and thermal energy fluxes from the southern Lakki plain, Nisyros (Greece). Geophys. Res. Lett. 28, 67–72.

Cardellini, C., Chiodini, G., Frondini, F., 2003. Application of stochastic simulations to CO_2 flux from soil: mapping and quantifying gas release. J. Geophys. Res. 108, 2425. doi:10.1029/2002JB002165.

Chiodini, G., Cioni, R., Guidi, M., Raco, B., Marini, L., 1998. Soil CO_2 flux measurements in volcanic and geothermal areas. Appl. Geochem. 13, 543–552.

Chiodini, G., Frondini, F., Cardellini, C., Granieri, D., Marini, L., Ventura, G., 2001. CO_2 degassing and energy release at Solfatara volcano, Campi Flegrei, Italy. J. Geophys. Res. 106 B8, 16213–16221.

Chiodini, G., Frondini, F., Raco, B., 1996. Diffuse emission of CO_2 from the Fossa crater, Vulcano Island (Italy). Bull. Volc. 58, 41–50.

Chiodini, G., Granieri, D., Avino, R., Caliro, S., Costa, A., Werner, C., submitted for publication. Carbon dioxide diffuse degassing: implications on the energetic state of volcanic/hydrothermal systems. J. Geophys. Res.

Clifton, A.E., Schlische, R.W., 2003. Fracture populations on the Reykjanes Peninsula, Iceland: comparison with experimental clay models of oblique rifting. J. Geophys. Res. 108 B2, 2074.

D'Amore, F., Truesdell, A.H., 1985. Calculations of geothermal reservoir temperatures and steam fractions from gas compositions. GRC Trans. 9, 305–310.

David, M., 1977. Geostatistical Ore Reserve Estimations. Elsevier, New York.

Dawson, G.B., 1964. The nature and assessment of heat flow from hydrothermal areas. N.Z. J. Geol. Geophys. 7, 155–171.

Deutsch, C.V., Journel, A.G., 1998. GSLIB: Geostatistical Software Library and Users Guide. Oxford University Press, New York.

Elmarsdóttir, Á., Ingimarsdóttir, M., Hansen, Í., Ólafsson, J.S., Magnússon, S., 2003. Vegetation and invertebrates in six high-temperature geothermal areas in Iceland. Icelandic Museum of Natural History and University of Iceland Institute of Biology report (in Icelandic).

Favara, R., Giammanco, S., Inguaggiato, S., Pecoraino, G., 2001. Preliminary estimate of CO_2 output from Pantelleria Island volcano (Sicily, Italy): evidence of active mantle degassing. Appl. Geochem. 16, 883–894.

Franz, G., Libscher, A., 2004. Physical and chemical properties of the epidote minerals – an introduction. In: Libscher, A., Franz, G. (Eds.), Reviews in Mineralogy and Geochemistry, vol. 56. Mineralogical Society of America and Geochemical Society, pp. 1–80.

Franzson H., 2004. Reykjanes high-temperature geothermal system. Geological and geothermal model. Iceland GeoSurvey report ÍSOR-2004/012 (in Icelandic).

Franzson H., Thordarson S., Björnsson G., Gudlaugsson S.Th., Richter B., Fridleifsson G.Ó., Thórhallsson S., 2002. Reykjanes high-temperature field SW-Iceland. Geology and hydrothermal alteration of well RN-10. In: Proceedings of the 27th Workshop Geothermal Reservoir Engineering, Stanford University.

Gerlach, T.M., McGee, K.A., Elias, T., Sutton, A.J., Doukas, M.P., 2002. Carbon dioxide emission rate of Kilauea Volcano: implications for primary magma and the summit reservoir. J. Geophys. Res. 107 B9, 2189.

Gíslason, S.R., 2000. Carbon dioxide from Eyjafjallajökull and chemical composition of spring water and river water in the Eyjafjalljökull – Mýrdalsjökull region. Science Institute, University of Iceland, Report RH-06-2000.

Granieri, D., Chiodini, G., Marzocchi, W., Avino, R., 2003. Continuous monitoring of CO_2 soil diffuse degassing at Phlegraean Fields (Italy): influence of environmental and volcanic parameters. Earth Plan. Sci. Lett. 212, 167–179.

Gudmundsdóttir, A.L., 1988. Natural heat flow through surface in geothermal areas in the Nesjavellir area. University of Iceland 4th year honors thesis.

Hernández, P.A., Notsu, K., Salazar, J.M., Mori, T., Natale, G., Okada, H., Virgili, G., Shimoike, Y., Sato, M., Pérez, N.M., 2001a. Carbon dioxide degassing by advective flow from Usu volcano, Japan. Science 292, 83–86.

Hernández, P.A., Perez, N.M., Salazar, J.M., Nakai, S., Notsu, K., Wakita, H., 1998. Diffuse emissions of carbon dioxide, methane, and helium-3 from Teide volcano, Tenerife, Canary Islands. Geophys. Res. Lett. 25, 3311–3314.

Hernández, P.A., Salazar, J.M., Shimoike, Y., Mori, T., Notsu, K., Pérez, N.M., 2001b. Diffuse emissios of CO_2 from Miyakejima volcano, Japan. Chem. Geol. 177, 175–185.

Jakobsson, S.P., Jónsson, J., Shido, F., 1978. Petrology of the Western Reykjanes Peninsula, Iceland. J. Petrol. 19, 669–705.

Johnson, J.W., Oelkers, E.H., Helgeson, H.C., 1992. SUPCRT92 – a software package for calculating the standard molal thermodynamic properties of minerals, gases, aqueous species, and reactions from 1 bar to 5000 bar and 0 °C to 1000 °C. Comput. Geosci. 18, 899–947.

Jónsson, J., 1968. Changes in the geothermal area at Reykjanes in 1967. National Energy Authority Report 10421 OST 5 (in Icelandic).

Jónsson, J., 1983. Historic eruptions on the Reykjanes Peninsula. Náttúrufraedingurinn 52, 127–139 (in Icelandic).

Karlsdóttir, R., 2005. TEM-measurements at Reykjanes 2004. Iceland GeoSurvey Report ÍSOR-2005/002 (in Icelandic).

Kerrick, D.M., 2001. Present and past nonanthropogenic CO_2 degassing from the solid Earth. Rev. Geophys. 39, 564–585.

Lewicki, J.L., Connor, C., St-Amand, K., Stix, J., Spinner, W., 2003. Self-potential, soil CO_2 flux and temperature on Masaya volcano, Nicaragua. Geophys. Res. Lett. 30, 1817.

Lonker, S.W., Franzson, H., Kristmannsdóttir, H., 1993. Mineral–fluid interactions in the Reykjanes and Svartsengi geothermal systems, Iceland. Am. J. Sci. 293, 605–670.

Marty, B., Tolstikhin, I.N., 1998. CO_2 fluxes from mid-ocean ridges, arcs and plumes. Chem. Geol. 145, 233–248.

Mörner, N.A., Etiope, G., 2002. Carbon degassing of the lithosphere. Global Planet. Change 33, 185–203.

Nehring, N.L., D'Amore, F., 1984. Gas chemistry of the Cerro Prieto, Mexico. Geothermics 13, 75–89.

Notsu, K., Sugiyama, K., Hosoe, M., Uemura, A., Shimoike, Y., Tsunomori, F., Sumino, H., Yamamoto, J., Mori, T., Hérnandez, P.A., 2005. Diffuse CO_2 efflux from Iwojima volcano, Izu-Ogasawara arc, Japan. J. Volc. Geoth. Res. 139, 147–161.

Óskarsson, N., 1996. Carbon dioxide from large volcanic eruptions. Short term effects. In: Biological Society of Iceland.

The carbon budget of Iceland Conference, Reykjavík 22–23 November 1966. Prog. and Abstr., p. 17 (In Icelandic).

Pálmason, G., Saemundsson, K., 1974. Iceland in relation to Mid-Atlantic Ridge. Ann. Rev. Earth Plan. Sci. 2, 25–50.

Pálmason, G., Johnsen, G.V., Torfason, H., Sæmundsson, K, Ragnars, K, Haraldsson, G.I., Halldórsson, G.K., 1985. Assessment of geothermal energy in Iceland. Orkustofnun OS-85076/JHD-10.

Saemundsson, K., Jóhannesson, H., 2004. Geothermal map of Iceland. Iceland GeoSurvey and Icelandic Energy Authority.

Saemundsson, K., Thórhallsson, S., Björnsson, G., Karlsdóttir, R., Franzson, H., 2004. Siting of drillholes RN-17 to RN-21 at Reykjanes. Iceland GeoSurvey report ÍSOR-04088 (in Icelandic).

Salazar, J.M.L., Hernándes, P.A., Pérez, N.M., Melián, G., Álvarez, J., Segura, F., Notsu, K., 2001. Diffuse emission of carbon dioxide from Cerro Negro volcano, Nicaragua, Central America. Geophys. Res. Lett. 28, 4275–4278.

Sapper, K., 1908. On some Icelandic volcanic fissures and crater rows. Neu. Jahrb. Min. Geol. Paläontol., 26 (in German).

Schmidt, E., Grigull, U., 1979. Properties of Water and Steam in SI-units: 0–800 °C, 0–1000 bar. Springer-Verlag, Berlin Heidelberg, R. Oldebourg, München.

Sigurgeirsson, M.Á., 1995. The younger Stampar eruption at Reykjanes. Náttúrufraedingurinn 64, 211–230 (in Icelandic).

Sigurgeirsson, M.Á., 2004. A chapter in the eruption history of Reykjanes: eruption episode two thousand years ago. Náttúrufraedingurinn 72, 21–28 (in Icelandic).

Sinclair, A.J., 1974. Selection of threshold values in geochemical data using probability graphs. J. Geochem. Explor. 3, 129–149.

Sorey, M.L., Colvard, E.M., 1994. Measurements of heat and mass flow from thermal areas in Lassen Volcanic National Park, California, 1984–1993. U.S.G.S. Water Resour. Invest. Rep., 94–4180-A.

Stefánsson, A., Arnórsson, S., 2002. Gas pressures and redox reactions in geothermal fluids in Iceland. Chem. Geol. 190, 251–271.

Sutton, O.G., 1953. Micrometeorology. McGraw-Hill, New York.

Sveinbjörnsdóttir, A.E., 1991. composition of geothermal minerals from saline and dilute fluids – Krafla and Reykjanes, Iceland. Lithos 27, 301–315.

Thorkelsson, Th., 1928. On thermal activity in Reykjanes. Rit Vísindafélags Íslendinga, 3.

Werner, C., Brantley, S., 2003. CO_2 emissions from the Yellowstone volcanic system. Geochem. Geophys. Geosyst. 4, 1061.

Werner, C., Brantley, S.L., Boomer, K., 2000. CO_2 emissions related to the Yellowstone volcanic system 2. Statistical sampling, total degassing, and transport mechnanisms. J. Geophys. Res. 105, 10831–10846.

Werner, C., Christenson, B.J., Scott, K., Britten, K., Kilgour, G., 2004. Monitoring CO_2 emissions at White Island volcano, New Zealand: evidence for total decrease in magmatic mass and heat output. In: Wanty R.B., Seal II R.R. (Eds.), Proceedings of the 11th International Symposium Water–Rock Interaction, WRI-11, pp. 223–226.

Wolfe, C.J., Bjarnason, I.Th., VanDecar, J.C., Solomon, S.C., 1997. Seismic structure of the Iceland mantle plume. Nature 385, 245–247.

Zhao, Ping, Ármannsson, H., 1996. Gas geothermometry in selected Icelandic geothermal fields with comparative examples from Kenya. Geothermics 25, 307–347.